Pattern of x-ray scattering by thermal phonons in Si

Z. Wu
Frederick Seitz Materials Research Laboratory, University of Illinois at Urbana-Champaign, 104 South Goodwin Avenue, Urbana, Illinois 61801-2902
and Department of Materials Science and Engineering, University of Illinois at Urbana-Champaign, 1304 West Green Street, Urbana, Illinois 61801-2980

Hawoong Hong
Frederick Seitz Materials Research Laboratory, University of Illinois at Urbana-Champaign, 104 South Goodwin Avenue, Urbana, Illinois 61801-2902

R. Aburano*
Frederick Seitz Materials Research Laboratory, University of Illinois at Urbana-Champaign, 104 South Goodwin Avenue, Urbana, Illinois 61801-2902
and Department of Physics, University of Illinois at Urbana-Champaign, 1110 West Green Street, Urbana, Illinois 61801-3080

P. Zschack and P. Jemian
Frederick Seitz Materials Research Laboratory, University of Illinois at Urbana-Champaign, 104 South Goodwin Avenue, Urbana, Illinois 61801-2902

J. Tischler
Solid State Division, Oak Ridge National Laboratory, Oak Ridge, Tennessee 37831-6033

Haydn Chen
Frederick Seitz Materials Research Laboratory, University of Illinois at Urbana-Champaign, 104 South Goodwin Avenue, Urbana, Illinois 61801-2902
and Department of Materials Science and Engineering, University of Illinois at Urbana-Champaign, 1304 West Green Street, Urbana, Illinois 61801-2980

D.-A. Luh and T.-C. Chiang†
Frederick Seitz Materials Research Laboratory, University of Illinois at Urbana-Champaign, 104 South Goodwin Avenue, Urbana, Illinois 61801-2902
and Department of Physics, University of Illinois at Urbana-Champaign, 1110 West Green Street, Urbana, Illinois 61801-3080
(Received 10 April 1998; revised manuscript received 15 May 1998)

Intensity distribution of x-ray scattering by thermal phonons in Si was recorded using synchrotron undulator radiation. A high-energy beam sent through a Si(111) wafer in a transmission Laue geometry yielded a threefold symmetric pattern for the scattering cross section with rich details governed by phonon dispersion, population, and polarization. [S0163-1829(99)08105-9]

Phonons in solids are usually probed by neutron scattering because the energy-momentum relationship for neutrons is well matched to typical phonon dispersion curves.[1] This is not the case for x-ray photons. To access the entire Brillouin zone by scattering, the probe particle must have a sufficiently large momentum. This means a large energy for photons, in the 10^4-eV range. To detect the energy loss by a phonon-scattering event, energy resolution on the order of 10^{-2} eV, or better, is required. The resolving power required for the spectrometer is thus $10^4/10^{-2}=10^6$, making this a rather difficult experiment. Despite recent advances in x-ray instrumentation including the development of new third-generation storage rings and insertion devices, the required high resolving power remains an obstacle to widespread application of x-ray scattering to phonon studies. Yet, x-ray scattering remains attractive, and in fact, it is the only option for materials with a high neutron absorption cross section. Other advantages include a much better momentum resolution, a minimal requirement on sample volume, and the possibility of energy tuning through absorption edges for elemental contrast in complex materials. The present study is a demonstration of a new approach to x-ray scattering by phonons using Si as a model test system. Instead of resolving both momentum and energy for the scattering event, we concentrate on momentum resolution only, and compensate the lack of energy resolution by area detection. The result is an intensity pattern directly proportional to a phonon-scattering cross section that contains information about phonon dispersion, population, and polarization. This approach is highly efficient, as the entire pattern covering several zones can be recorded in a matter of minutes using undulator radiation at the Advanced Photon Source. The results provide a simple

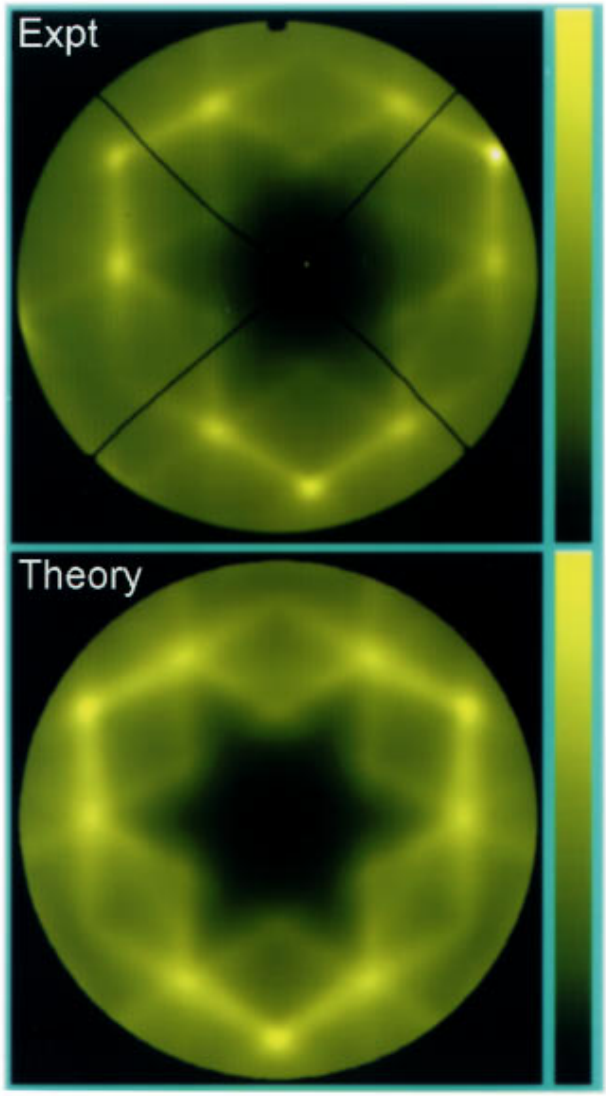

FIG. 1. (Color) Experimental and theoretical phonon-scattering patterns showing the logarithmic scattering intensity. The bar on the right shows the intensity levels used for display on a linear scale.

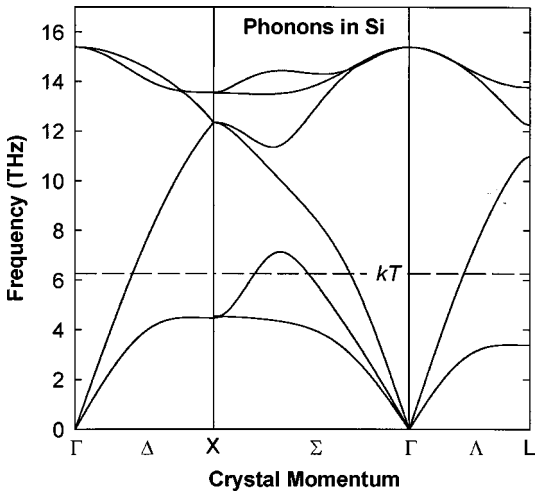

FIG. 2. Phonon dispersion curves of Si. The horizontal dashed line corresponds to kT at room temperature.

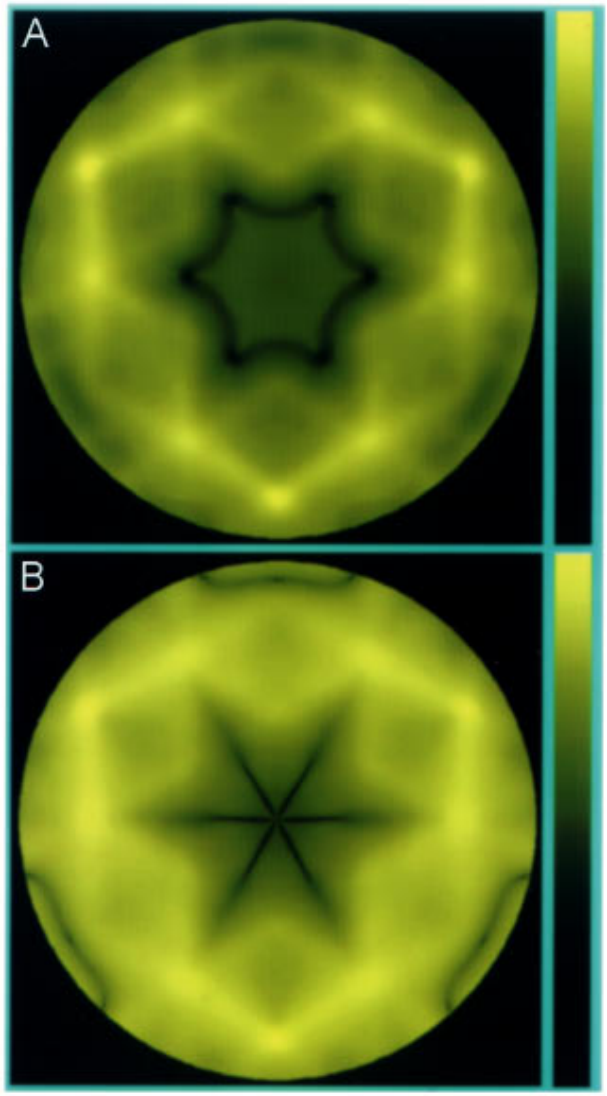

FIG. 3. (Color) (a) Theoretical phonon-scattering pattern with the optical phonons ignored. (b) Theoretical phonon-scattering pattern with only the two TA branches included in the calculation.

and effective visualization of the anisotropy and intricate details of the intensity distribution associated with phonon scattering.

Our experiment was carried out at the undulator beamline of Sector 33 (the UNICAT sector) at the Advanced Photon Source. A double-crystal monochromator was used to select an x-ray energy of 28 keV. A transmission Laue geometry was employed, in which the monochromatic beam was sent at near normal incidence through a commercial Si(111) wafer with a thickness of about 0.4 mm. The detector, either a type-57 Polaroid film (with no phospher screen) or an image plate, was positioned behind the sample at a distance ranging from 30 to 60 cm. The sample was enclosed in a vacuum chamber equipped with Be windows for the incident and scattered radiation. The vacuum environment was necessary for reducing air scattering. Each image required an exposure time of several minutes. The images obtained from the image plate and the film looked the same.

The top panel in Fig. 1 shows a typical pattern recorded on an image plate. The only adjustment made to the image is

a uniform background subtraction and intensity normalization to span the full scale of the display. The bar on the right of the image shows the mapping of intensity levels to a linear scale. Only a circular portion of the image plate was exposed, which corresponds to the circular shape of the exit Be window of the vacuum chamber. The four black lines emanating from the center of the picture are shadows of four wires in the vacuum chamber used for supporting a direct-beam stop. The beam stop, made of 2-mm-thick Mo, does not completely stop the direct beam, and the remnant of the incident beam gives rise to a very small white dot at the center of the picture.

None of the scattering features seen in Fig. 1 are due to Bragg diffraction by the crystal lattice. The Ewald sphere has a shell of essentially zero thickness with our monochromatic beam, and the choice of the x-ray energy and scattering geometry is such that this shell does not intersect any of the reciprocal lattice points. The pattern is thus entirely due to phonon scattering. Since the image plate has a logarithmic output, the pattern seen in Fig. 1 is a direct measure of the phonon-scattering cross section on a logarithmic scale as a function of momentum transfer. The momentum transfer is zero at the center of the picture, and increases towards the edge of the picture. The main component of the momentum transfer is within the plane of the Si sample, but there is also a significant perpendicular component away from the center of the picture due to the finite radius of the Ewald sphere. The sample is slightly misaligned; otherwise, the pattern exhibits an apparent threefold symmetry.[2]

The bottom panel in Fig. 1 shows the result of our calculation of the expected phonon-scattering pattern. In this calculation, only one-phonon scattering events are included, and the formula for the scattered intensity is[3]

$$I \propto f^2 e^{-2M} \sum_{j=1}^{6} \left[\frac{1}{\exp(\hbar\omega_j/kT)} + \frac{1}{2} \right] \frac{|\mathbf{q}\cdot\hat{\mathbf{e}}_j|^2}{\omega_j}, \qquad (1)$$

where f is the atomic scattering factor,[3] M is the Debye-Waller factor,[4] ω is the phonon frequency, $\mathbf{q}$ is the momentum transfer, which is also the momentum of the scattered phonon in extended zone, $\hat{\mathbf{e}}$ is the phonon polarization vector, and T is the temperature of the sample (room temperature). The quantities f, M, ω, and $\hat{\mathbf{e}}$ are dependent on $\mathbf{q}$. The temperature enters the formula through the phonon population factor. The summation is over the six phonon branches in Si (three acoustic and three optical). Higher-order scattering, being much weaker and backgroundlike, is ignored in our calculation. The phonon-dispersion curves of Si used in this calculation, shown in Fig. 2, are obtained by a fit to available neutron-scattering data.[5] The theoretical pattern in Fig. 1 is displayed using the same logarithmic scale as the experimental data; namely, it is a plot of

$$\frac{\ln(I) - \ln(I_{\min})}{\ln(I_{\max}) - \ln(I_{\min})}. \qquad (2)$$

As seen in Fig. 1, the theoretical pattern is in good agreement with the experimental results. The main features of the pattern are explained in the following. Equation (1) contains a factor of $1/\omega$; thus, the scattering intensity is generally dominated by low-energy acoustic phonons. This energy bias is further amplified by the thermal population factor, which also goes like $1/\omega$ in the limit of small ω. The horizontal dashed line in Fig. 2 corresponds to kT at room temperature, and it is clear that the optical phonons will generally contribute much less to the intensity. The combined effect is a $1/\omega^2$ asymptotic dependence, which should diverge at the zone center. The center of the pattern corresponds to $q=0$, where $\omega \to 0$ for the acoustic modes. The $1/\omega^2$ singularity is, however, compensated by the q^2 factor in Eq. (1), and the intensity remains finite ($\omega = \nu q$ near the zone center, where ν is the sound velocity). The pattern is quite dark near the center because the polarization factor in Eq. (1) vanishes for the transverse modes.

As the scattering vector $\mathbf{q}$ increases towards the edge of the picture, it moves beyond the first Brillouin zone and can become close to a reciprocal lattice point. This is equivalent to being near the zone center by umklapp, and the acoustic modes, with low ω values, will give rise to high intensities because of the $1/\omega^2$ dependence mentioned above (now q remains finite). This accounts for the nine intense spots near the edge of the circle of exposure seen in Fig. 1. The intensity does not diverge, because the Ewald sphere does not actually intersect any reciprocal lattice points. The three outer spots are relatively more intense and correspond to points on the Ewald sphere closest to $(\overline{1}13)$ and its equivalent reciprocal lattice points. The other six spots correspond to $(0\overline{2}2)$ and its equivalent reciprocal lattice points.

These spots can also be labeled in terms of the standard hexagonal surface coordinate system used extensively by the surface diffraction community.[6] The three brighter, outer spots correspond to $(0\overline{2})$-type ''rods,'' and the other six spots correspond to $(1\overline{2})$-type ''rods.'' The six bright line segments connecting these intense spots lie approximately along $[1\overline{1}1]$ and its equivalent directions in cubic notation. Figure 2 shows that the transverse acoustic (TA) phonons are ''soft'' along [111]; namely, for a given q, they have the lowest frequency along [111] than all other crystallographic directions. This low frequency gives rise to the observed high intensity along the line segments. The longitudinal acoustic phonons are unimportant in this discussion because of their higher frequencies and the polarization factor in Eq. (1). The other weaker features in the pattern can be explained similarly.

The logarithmic scale used in Fig. 1 compresses the intensity and brings out details that are invisible to the eye if a linear scale is used. Thus, the logarithmic pattern is a very sensitive test for theoretical modeling. To illustrate this sensitivity, we show in Fig. 3(a) a theoretical pattern calculated in the same way as before but with the three optical branches ignored. The normalization of the pattern is again based on Eq. (2), and since $I_{\min}$ is different, the overall normalization is different from that of Fig. 1. As mentioned above, the thermal population factor and the $1/\omega$ factor make the contribution from the optical phonon modes relatively unimportant. Indeed, a linear-scale plot shows no discernable differences. But the logarithmic pattern shown in Fig. 3(a) is clearly different. While the most intense features in the pattern remain the same (dominated by acoustic modes), the details of the pattern in the low intensity areas have changed dramatically. In particular, six dark spots have emerged,

which are not seen in the experiment, and the center of the pattern no longer exhibits the lowest intensity. Likewise, Fig. 3(b) is a theoretical pattern with only the two TA modes retained in the calculation, which further illustrates the types of pattern changes that can occur if a simplified model is employed. Near the center of the picture, the TA modes contribute little to the intensity because of the polarization factor in Eq. (1), and ignoring the longitudinal acoustic mode should have a large effect here, as seen in the calculation. The sensitivity illustrated above suggests that the logarithmic pattern is a useful tool for detailed analyses of phonon properties of solids. A close analogy is the x-ray truncation rod method commonly employed for surface structural determination, where the intensity analysis is also carried out on a logarithmic scale.[6] By this analogy, it can be inferred that an experimental intensity pattern such as the one shown in Fig. 1 can be used to determine phonon-dispersion curves via a least-squares analysis for materials where such information is needed. The simple experimental geometry, a fast data acquisition rate, and a minimal requirement on sample volume could make this technique a valuable complement to neutron scattering.

To summarize, the present experiment is a demonstration of a new approach for phonon studies. Using Si as a model test system, a transmission x-ray Laue pattern is recorded to yield the scattering cross section as a function of momentum transfer. The intensity pattern, displayed on a logarithmic scale, shows features that are sensitive to details of the phonon properties. This approach (and its extension to include temperature-dependent measurements) should be useful for investigations of a variety of materials. Phase transitions involving phonons are a potential area of interest.

This work was supported by the U.S. Department of Energy (Division of Materials Sciences, Office of Basic Energy Sciences) under Grant No. DEFG02-91ER45439. Acknowledgments are also made to the Donors of the Petroleum Research Fund, administered by the American Chemical Society, and to the U.S. National Science Foundation Grants No. DMR-95-31582 and No. DMR-95-31809 (T.C.C.) for partial equipment support in connection with the synchrotron beamline operation. The UNICAT facility at the APS is supported by the University of Illinois Frederick Seitz Materials Research Laboratory, the State of Illinois IBHE/HECA program, the Oak Ridge National Laboratory (U.S. Department of Energy Contract No. DE-AC05-96OR22464), the National Institute of Science and Technology (U.S. Department of Commerce), and UOP R&D Corp. The APS is supported by the U.S. Department of Energy (Basic Energy Sciences) under Contract No. W-31-109-ENG-38. We wish to thank DND-CAT for the use of their image plate reader.

*Present address: Cypress Semiconductor, 3901 North First Street, San Jose, CA 95134.

†Author to whom correspondence should be addressed. Electronic address: ⟨t-chiang@uiuc.edu⟩

[1] G. P. Srivastava, *The Physics of Phonons* (Adam Hilger, New York, 1990).

[2] One might expect a sixfold pattern because of the inversion symmetry of the Si(111) lattice. However, this inversion symmetry is broken by the scattering geometry.

[3] B. E. Warren, *X-Ray Diffraction* (Dover, New York, 1969). X-ray scattering by thermal phonons is often referred to as thermal diffuse scattering. Our Eq. (1) is a straightforward generalization of Warren's Eq. (11.35) to the case of two identical atoms in a unit cell. The dot product of $\mathbf{q}$ and $\hat{\mathbf{e}}_j$ in our Eq. (1) gives rise to a cosine factor, which is shown explicitly in Warren's Eq. (11.35). The average thermal energy for each mode $\langle E_{gj} \rangle$ in Warren's equation is given explicitly by Eq. (11.21) in the same reference. With these substitutions, the readers can easily verify that our Eq. (1) has the same form as Warren's Eq. (11.35), except that the summation is now over six modes for each $\mathbf{q}$ instead of three because of the two-atom basis.

[4] M. Deutsch and M. Hart, Phys. Rev. B **31**, 3846 (1985).

[5] F. Herman, J. Phys. Chem. Solids **8**, 405 (1959). An error in this work was pointed out in C. Patel, W. F. Sherman, and G. R. Wilkinson, J. Phys. C **17**, 6063 (1984). Our calculation extends the work of Patel *et al.*, to include up to the fifth neighbors.

[6] I. K. Robinson and D. J. Tweet, Rep. Prog. Phys. **55**, 599 (1992); R. G. van Silfhout, J. F. van der Veen, C. Norris, and J. E. Macdonald, Faraday Discuss. Chem. Soc. **89**, 169 (1990).